Journal of Power Sources 243 (2013) 233–241

Contents lists available at SciVerse ScienceDirect

Journal of Power Sources

journal homepage: www.elsevier.com/locate/jpowsour

Stable hydrogen production by methane steam reforming in a two zone fluidized bed reactor: Experimental assessment

L. Pérez-Moreno, J. Soler, J. Herguido*, M. Menéndez

Catalysis, Molecular Separations and Reactor Engineering Group (CREG), Aragon Institute for Engineering Research (I3A), University of Zaragoza, 50009 Zaragoza, Spain

HIGHLIGHTS

- Two zone fluidized bed reactor (TZFBR) is proposed for H_2 production by steam reforming of methane.
- A higher global yield to hydrogen has been observed in the TZFBR than conventional reactors.
- Working with the TZFBR there was no net coke formation.
- Better values of methane conversion were obtained, due to a better regeneration of the catalyst.

GRAPHICAL ABSTRACT

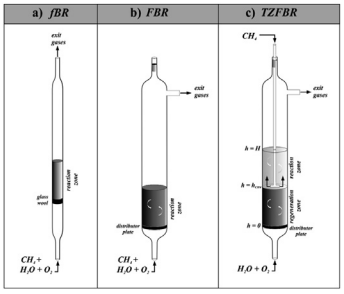

ARTICLE INFO

Article history:
Received 15 January 2013
Received in revised form
20 May 2013
Accepted 29 May 2013
Available online 13 June 2013

Keywords:
Oxidative steam reforming
Methane
Ni/Al_2O_3 catalyst
TZFBR
stability

ABSTRACT

The *Two Zone Fluidized Bed Reactor* concept is proposed for hydrogen production via the steam reforming of methane (SRM) including integrated catalyst regeneration. In order to study the effect of the contact mode, the oxidative SRM has been carried out over a Ni/Al_2O_3 catalyst using a fixed bed reactor (fBR), a conventional fluidized-bed reactor (FBR) and the proposed two-zone fluidized bed reactor (TZFBR). The technical feasibility of these reactors has been studied experimentally, investigating their performance (CH_4 conversion, CO and H_2 selectivity, and H_2 global yield) and stability under different operating conditions.

Coke generation in the process has been verified by several techniques. A stable performance was obtained in the TZFBR, where coke formation was counteracted with continuous catalyst regeneration. The viability of the TZFBR for carrying out this process with a valuable global yield to hydrogen is demonstrated.

1. Introduction

Natural gas reforming is the main source of hydrogen. The annual production of hydrogen is estimated at 400 billion m^3, North America being the most important producer (230 billion m^3) [1]. About 60% comes from natural gas reforming while the major part of the remaining 40% is produced from petroleum refining or naphtha reforming.

Steam methane reforming is an established technology for obtaining hydrogen for fuel cells and for the production of synthesis gas that can be used for the Fischer–Tropsch process to obtain methanol and dimethyl ether, using nickel supported catalysts [2]. However, there are two main problems in the steam reforming of methane: a) the reaction is endothermic and requires an external heating source; b) the nickel based catalysts require the use of high steam/methane ratios (3–3.5) in order to avoid coke formation that causes the deactivation of the catalyst [3].

* Corresponding author. Tel: +34 976762393; fax: +34 976762142.
E-mail address: jhergui@unizar.es (J. Herguido).

0378-7753/$ – see front matter © 2013 Elsevier B.V. All rights reserved.
http://dx.doi.org/10.1016/j.jpowsour.2013.05.197

Two alternatives have been studied in order to overcome these problems. The first is the reduction of the steam/methane ratio, which reduces the endothermic character of the reaction but which does not reduce the coke deposition. The second is the partial introduction of oxygen so that exothermic reactions take place (such as combustion or partial oxidation). The latter process, known as oxidative steam methane reforming (OSRM), is more efficient than conventional steam methane reforming. However, it also has some drawbacks such as 1) the formation of hot spots in the initial part of the bed [4], 2) the low activity of the nickel based catalysts due to the oxidation of the nickel metallic species, 3) selectivity loss and 4) coke formation in the final part of the bed due to the lack of oxygen [5].

In oxidative steam methane reforming, oxygen must be supplied to the reactor with the steam so that the steam methane reforming (endothermic, Eq. (1)) is combined with two exothermic reactions: methane combustion (Eq. (2)) and the partial oxidation of methane (Eq. (3)). In this way, the global process is autothermic.

$$CH_4 + H_2O \rightarrow CO + 3H_2 \qquad \Delta H_{298} = 206 \text{ kJ mol}^{-1} \tag{1}$$

$$CH_4 + 2O_2 \rightarrow CO_2 + 2H_2O \qquad \Delta H_{298} = -803 \text{ kJ mol}^{-1} \tag{2}$$

$$CH_4 + \tfrac{1}{2}O_2 \rightarrow CO + 2H_2 \qquad \Delta H_{298} = -36 \text{ kJ mol}^{-1} \tag{3}$$

Other reactions that can also occur in the process are the water gas shift reaction (WGS) (Eq. (4)) and dry reforming (Eq. (5)):

$$CO + H_2O \leftrightarrow CO_2 + H_2 \qquad \Delta H_{298} = -41 \text{ kJ mol}^{-1} \tag{4}$$

$$CH_4 + CO_2 \rightarrow 2CO + 2H_2 \qquad \Delta H_{298} = 247 \text{ kJ mol}^{-1} \tag{5}$$

1.1. Coke formation

The high temperatures associated with steam reforming for hydrogen production also favour coke formation. The deactivation of nickel catalysts by carbon deposition is a significant problem in methane reforming caused by fouling of the Ni surface, blockage of the pores of the catalytic particles and disintegration of the support material [6]. Any measure resulting in the reduction of coke formation presents a significant economic advantage for the process. For this reason, the formation and elimination of coke remains an interesting topic.

Thermodynamically, the most feasible reactions for carbon formation are the following:

$$CH_4 \leftrightarrow C + 2H_2 \text{ (}CH_4\text{ cracking)} \qquad \Delta H_{298} = 122.3 \text{ kJ mol}^{-1} \tag{6}$$

$$2CO \leftrightarrow C + CO_2 \text{ (Boudouard)} \qquad \Delta H_{298} = -125.2 \text{ kJ mol}^{-1} \tag{7}$$

$$CO + H_2 \leftrightarrow C + H_2O \text{ (CO reduction)} \qquad \Delta H_{298} = -84.0 \text{ kJ/mol} \tag{8}$$

The yield for each reaction mainly depends on the temperature of the process. Coke formation from reactions (7) and (8) is less favoured when the temperature increases. However, coke formation through reaction (6) rises considerably at higher temperatures.

Minimisation of coking is one of the major factors governing the industrial application of steam reforming [7]. The thermodynamics of the process mean that reaction conditions that favour coke formation cannot be avoided, but operating conditions can be chosen to minimise coke. An example is increasing the steam/methane ratio in order to favour the gasification of carbon with steam (i.e. the reverse reaction of CO reduction).

Coke may be deposited on the nickel catalyst in various forms, all of which have unique characteristics and differences in reactivity [8]. This carbon formation, specifically under steam reforming conditions, may occur through three routes that result in different kinds of coke. At temperatures lower than 500 °C, adsorbed hydrocarbons may accumulate on the nickel surface and slowly polymerize into an encapsulating film, blocking and deactivating the nickel surface. At temperatures above 600 °C, pyrolytic coke formed by the thermal cracking of hydrocarbons may encapsulate and deactivate the catalyst particles. At temperatures higher than 450 °C, whisker carbon is the main product of carbon formation via a mechanism involving the diffusion of carbon through nickel crystals, nucleation, and whisker growth with a nickel crystal on the top. The whisker type carbon does not deactivate the nickel surface but can cause a breakdown of the catalyst by pore plugging.

1.2. Catalysts

For the oxidative steam methane reforming reaction, Ni-supported catalysts have mainly been used. In fact, the development of Ni catalysts for this process has been extensively studied [9–13]. Ni catalysts are cheaper and more readily available than noble metal based catalysts such as Pt and Rh. However, Ni-catalysts are easily deactivated in oxidative methane reforming due to the oxidation of the metallic species of Ni. Another problem with this process is the formation of hot spots. It has been reported that Rh and Pd based catalysts are effective for eliminating this hot spot formation [14–16], while Ni based catalysts tend to form these hot spots in the bed of the catalyst [13–15,17]. Nevertheless, noble metals such as Pt, Pd and Rh are not suitable components due to their limited availability and their high price. For this reason Ni-based catalysts have been more intensely studied in recent years by several authors [18–25]. In these works, Ni-based catalysts were doped with low quantities of noble metals. The intention was to achieve a high degree of resistance to the formation of hot spots by means of combining the high activity of nickel with the high reducibility of the noble metals.

1.3. Reactors

The use of the two-zone fluidized bed reactor (TZFBR) [26] could serve to prevent the aforementioned problems of oxidative steam methane reforming from occurring. With this reactor configuration, activity losses are not expected because regeneration takes place simultaneously with the reaction in the same vessel. The circulation of the solid particles in the fluidized bed would mean that its behaviour was that of an isothermal bed, avoiding the formation of hot spots. At the same time, the heat production in the regeneration step (i.e. coke combustion) would compensate for the endothermicity of the steam reforming. Moreover, it would be possible to reduce the steam/methane ratio (S/M) because the coke deposition problem associated with low S/M values is counteracted by its simultaneous regeneration.

This type of reactor consists of a fluidized bed where the oxygen–steam mixture is fed through the lower part of the reactor, while the methane is introduced at an intermediate point of the bed height. In this way, two zones are created in the reactor: in the lower part the greater part of the oxygen is consumed reacting with the reduced catalyst (regeneration zone), while in the upper part the desired chemical reaction takes place (reaction zone). The circulation of the solid between both zones enables a steady state to be achieved. This reactor allows the continuous regeneration of the catalyst, avoiding the transfer of large amounts of solid between reactors because a single vessel is used. There are two critical issues regarding the operation of a TZFBR. On the one hand, the gas phase oxygen must be consumed in the lower part of the reactor

(although in some cases it may be desirable to maintain a small oxygen concentration in the hydrocarbon-rich zone); on the other hand, the backmixing of gases must be avoided, especially of the hydrocarbon [26].

The TZFBR was developed by the Catalysis and Reactor Engineering Group (CREG) with the purpose of operating in continuous mode using a single reactor. It was first proposed for oxidative coupling of methane [27]. This verified the feasibility of the system. The applicability of this reactor to reactions where coke formation causes the deactivation of the catalyst was demonstrated in a study of the dehydrogenation of butane in a TZFBR by Callejas et al. [28]. In recent years the viability of the use of this type of reactor for different processes has been evaluated, for example in catalytic dehydrogenation processes including propane dehydrogenation using a Pt–Sn–K/γ-Al_2O_3 catalyst [29] and n-butane dehydrogenation using a Pt–Sn/$MgAl_2O_4$ catalyst [30]. In both processes it was concluded that the TZFBR is useful for its application in the dehydrogenation of alkanes, the operational conditions being very important for the performance of the process. These conditions need to be optimized in order to achieve equilibrium between the velocity of coke formation (in the reaction zone) and the velocity of coke combustion (in the regeneration zone). This reactor has recently been successfully tested for oxidative steam reforming of ethanol [31] obtaining stable results and continuous operation without net catalyst deactivation.

This work examines the feasibility of achieving stable SRM in a TZFBR and analyses the improvements made with the use of this TZFBR in the OSRM in order to obtain hydrogen and carbon monoxide from methane while avoiding the usual problems of this process. Experiments using a Ni-based catalyst have been carried out in a fixed bed reactor (fBR), a conventional fluidized bed reactor (FBR) and a TZFBR in order to compare the performance of these different types of contact mode configurations.

2. Experimental

2.1. Catalyst preparation

A commercially available γ-Al_2O_3 particulate solid (Sigma–Aldrich; $S_{BET} = 155\ m^2\ g^{-1}$; 150 mesh) was calcined at 950 °C in a muffle furnace for 1 h (heating rate = 10 °C min^{-1}) and used as the catalyst support material. The support thus obtained had a specific area of 76 $m^2\ g^{-1}$. The catalyst was prepared by incipient impregnation of this support material with an aqueous solution of the nickel precursor $Ni(NO_3)_2 \cdot 6H_2O$ (99.999%; Sigma–Aldrich). The resulting product was dried in an oven at 120 °C for 24 h. Subsequently, the sample was calcined at 950 °C in a muffle furnace for 1 h ($S_{BET} = 59\ m^2\ g^{-1}$). After calcination, the solid was sieved between 45 and 150 μm. Prior to work in reaction, catalyst was reduced at 800 °C for 2 h in a 10% H_2/N_2 stream.

2.2. Reaction

The reactor used for the fBR experiments consists of a 1.2 cm i.d. tube made of quartz, of 30 cm length, inside of which the catalyst is supported by glass wool (inert material) that acts as the gas distributor (Fig. 1a). The experimental system used for the FBR and TZFBR tests consists of a 2.8 cm i.d. fluidized bed reactor made of quartz, with a distributing porous plate of quartz (Fig. 1b and c). In the co-feeding configuration (i.e., in the fixed bed reactor and in the conventional fluidized bed reactor) the three reagents are introduced through the lower part of the bed (Fig. 1a and b). In the case of the TZFBR, a 0.4 cm o.d. quartz tube is inserted in the reactor in order to feed the methane at an intermediate point of the bed height (h_{CH_4}) while oxygen and steam are fed through the lower part (Fig. 1c). In all configurations, the temperature was measured by means of a thermocouple located into the catalytic bed.

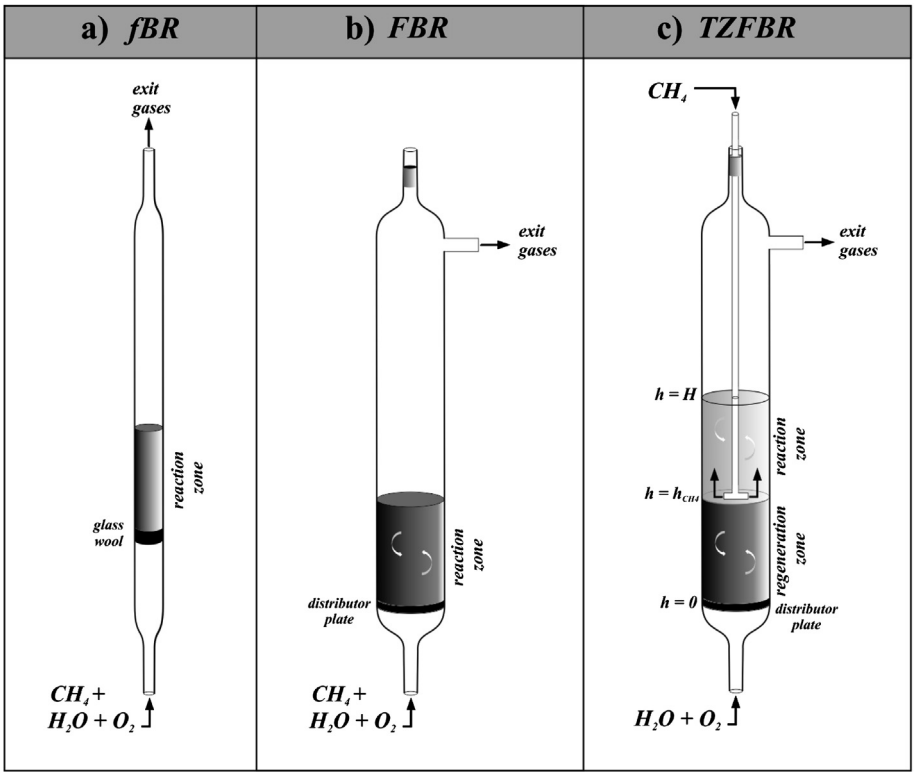

Fig. 1. Diagram of the reactor configurations: a) fixed bed reactor, b) traditional fluidized bed reactor and c) two zone fluidized bed reactor.

The gaseous reagents are fed by means of mass flow controllers (model 5850 TR, Brooks Instruments). The water is fed through an HPLC pump (Shimadzu; model LC-10AT VP) to a vaporizer heated at 150 °C after which the steam stream and the oxygen stream is mixed. Water is condensed from the product stream in a bath with salt and ice, while the non-condensed gases are analyzed by GC-TCD (Varian, CP-3800).

The following parameters were defined to calculate the performance of the process: conversion of methane (X_{CH_4}) and selectivity from methane to product i (S_i).

$$X_{CH_4}(\%) = \frac{100\cdot\left(F^{in}_{CH_4} - F^{out}_{CH_4}\right)}{F^{in}_{CH_4}} \quad (9)$$

$$S_i(\%) = \frac{100\cdot n_i F^{out}_i}{\left(F^{in}_{CH_4} - F^{out}_{CH_4}\right)} \quad (10)$$

$$S_{H_2}(\%) = \frac{100\cdot F^{out}_{H_2}}{3\left(F^{in}_{CH_4} - F^{out}_{CH_4}\right)} \quad (11)$$

A last parameter, the global yield to hydrogen from methane plus water ($Y_{H_2/(EtOH+H_2O)}$), was intended to evaluate the efficiency of both raw materials (methane and water) also taking into account the efficiency in the use of water.

$$Y_{H_2/(CH_4+H_2O)} = \frac{F^{out}_{H_2}}{2F^{in}_{CH_4} + F^{in}_{H_2O}} = \frac{F^{out}_{H_2}}{(2 + S/M)\cdot F^{in}_{CH_4}} \quad (12)$$

2.3. Catalyst characterization

Specific surface areas (BET) of the samples freshly calcined and after reaction in the different types of reactor were obtained by static N_2 adsorption measurements with TriStar 3000 (V6.08 A) equipment on samples previously degassed at 200 °C for 12 h. This equipment has a limit of detection of 0.01 $m^2\ g^{-1}$ and uses nitrogen–helium mixtures as adsorbate.

XRD patterns were obtained using a Rigaku/Max System diffractometer Cu (Model D/max 2500) equipped with a graphite monochromator. The step size was 0.03° with 2θ scanning from 5° to 80°.

Temperature-programmed reduction (TPR) experiments were carried out using AUTOCHEMII equipment (Micromeritics). The test conditions were: 1) drying of the sample with an argon flow of 50 N ml min^{-1} until 110 °C (heating rate 10 °C min^{-1}), and maintaining the temperature for 30 min; 2) reduction of the sample with a 10% H_2/Ar flow until 950 °C (heating rate 5 °C min^{-1}).

The surface morphology of the fresh and used catalysts was analyzed by transmission electron microscopy (TEM) on a JEOL 2000 FXII (200 kV) unit. The sample was dispersed in ethanol with an ultrasound bath for some minutes and then placed on a copper grill.

3. Results and discussion

3.1. SRM in fixed bed reactor

Several authors have reported coke formation when using a fixed-bed reactor in oxidative steam methane reforming, e.g. Nurunnabi et al. [5,32]. In Fig. 2, an example is shown of the time evolution of the selectivity to the different products, as well as the H_2/CO ratio obtained, using the fixed bed reactor facility. At the beginning of the experiment, the predominant reaction was the steam methane reforming reaction (Eq. (1)), obtaining a H_2/CO ratio close to 3. This ratio increased until t = 90 min after which there was a progressive decrease until the initial value was reached again. In these first 90 min there was also an increase in the selectivity to CO_2 and coke with a decrease in the selectivity to CO. This behaviour suggests that the CO formed in the steam methane reforming (Eq. (1)) and in the partial oxidation (Eq. (3)) reacts by means of the Boudouard reaction producing coke and CO_2 (Eq. (7)); and by means of the WGS reaction (Eq. (4)). After the first 90 min of time-on-stream, the catalyst deactivation was sharper, causing a rise in the selectivities to CO and coke, with a decrease in the selectivities to CO_2 and H_2. After the first 90 min, coke deposition also occurred. The most feasible explanation is that dry methane reforming (Eq. (5)) and the reverse of the WGS reaction (Eq. (4)) occurred and the Boudouard reaction (Eq. (7)) produced coke and CO_2. This could explain the decrease in the H_2/CO ratio and selectivity to hydrogen and the fact that coke was produced but with a decrease in the CO_2 selectivity. After 3 h of reaction, the product distribution was similar to that at the beginning of the process but with considerably lower activity (see next 3.2 section).

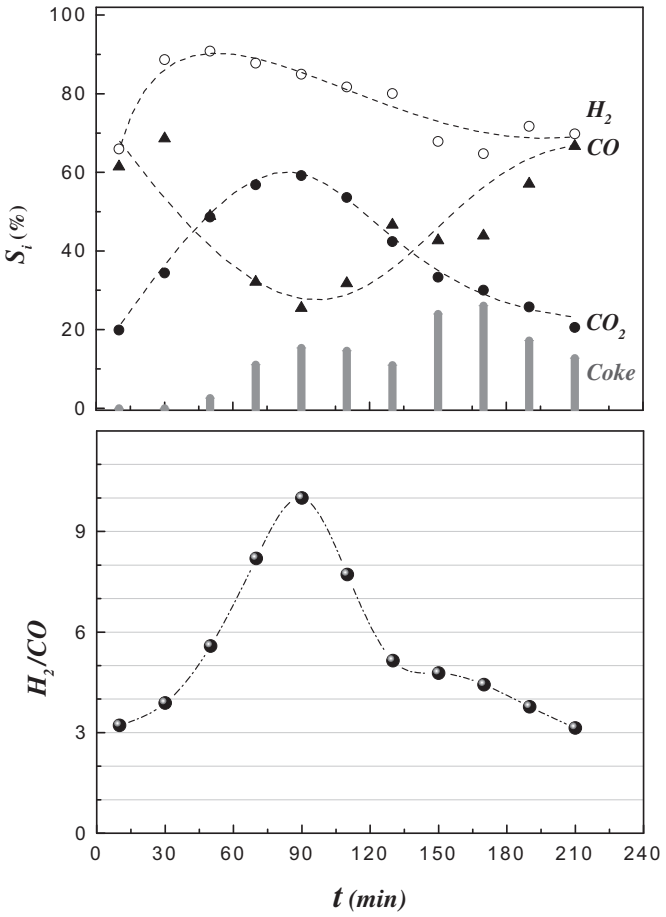

Fig. 2. Time evolution of methane conversion, selectivity to different products, and H_2/CO ratio in the gas product in the fixed bed reactor (lines for visual help). Operating conditions: T = 850 °C, W_{cat} = 1 g, $CH_4/H_2O/O_2$ = 2/1.5/1; W_{cat}/F = 0.67 g min $mmol^{-1}$. Coke is calculated by carbon mass balance closure.

Santos et al. (2010) studied the autothermal reforming of methane over an 8% Ni/α-Al_2O_3 catalyst at 800 °C and using $CH_4/H_2O/O_2$ = 2/0.4/1 [33]. These authors observed a similar effect to those observed in our study in a fixed bed reactor. CO and H_2 selectivities decreased with time due to the catalyst deactivation; while CO_2 selectivities showed the opposite behaviour. These

results were consistent with the so-called indirect mechanism usually applied for the partial oxidation of methane. In the first step, there is combustion of methane producing CO_2 and H_2O while in the second step H_2O and CO_2 reforming of unreacted methane takes place, forming H_2 and CO. In this way, when the catalyst deactivates, there is an inhibition of the second step of CO_2 reforming, causing a decrease in H_2 and CO selectivity and an increase in CO_2 selectivity, as occurred in the first 90 min of the study in the fixed bed reactor.

3.2. Study of the stability of the system

Pursuing stable operation by changing the reaction configuration, FBR and TZFBR have been used as alternatives to the conventional reactor (fBR). Fig. 3 shows a comparison between the activity (in terms of X_{CH_4}) in the fixed bed reactor, the FBR, and the TZFBR for oxidative steam methane reforming over Ni/Al_2O_3 catalysts; in order to check if there is catalyst deactivation over time. Under the experimental conditions of these tests, a considerable decrease in the conversion after the first 90 minutes was observed when the fBR was used, consistent with the previous results shown in Fig. 2. Fig. 3 shows the conversion evolution working with the FBR and the TZFBR under the same operating conditions. In the fixed bed reactor, which has a much smaller W/F ratio than the fluidized reactors, it is possible to obtain a greater conversion at the beginning of the experiment. There is less short circuit gas in this contact mode compared with the fluidized bed where the bubbles favour gas bypassing behaviour. However, the coke accumulation and the fact that there was no continuous regeneration produced a similar loss of activity in the fBR and FBR, as can be appreciated in Fig. 3.

The stable performance exhibited by the TZFBR results, even with the same W/F ratio as in the FBR, is indicative that a dynamic equilibrium between coke formation (in the upper zone of the reactor) and coke combustion (in the lower zone of the reactor) was reached in this reactor configuration. The steady state was achieved with a conversion very close to the thermodynamic equilibrium value (discontinuous horizontal line in Fig. 3).

However, the stationary state achieved with the TZFBR is totally reliant on the operating conditions. The methane/steam/oxygen feeding ratio is a key variable determining the final state. Fig. 4 shows the activity behaviour in the TZFBR for different steam to oxygen molar feeding ratios (S/O) at a constant methane/(steam + oxygen) value of 0.8. Although a stable state is attained for all S/O values, the lower the oxygen proportion in the feeding stream (high S/O values), the lower is the stationary methane conversion and the higher is the time-on-stream required to achieve this stationary state. This suggests that for high S/O values the amount of coke remaining on the catalyst surface in the stationary state (i.e., as a result of the dynamic equilibrium between coke formation and coke combustion processes) will be higher than when a greater proportion of feed oxygen is used. Accordingly, at very low oxygen feeding percentages there will be no steady state or else it will be achieved with very high coke content (i.e. very low catalyst activity). On the other hand, if the percentage of oxygen in the feed is too high, the amount of coke transferred from the reaction zone will not be enough to consume all the oxygen (this problem may also appear if the residence time in the lower zone is not enough, as will be discussed below). Some oxygen will then reach the upper zone where the combustion of methane, and of some SRM products, can occur. These undesirable reactions will decrease the selectivity and could result in a non-desired lower yield to hydrogen.

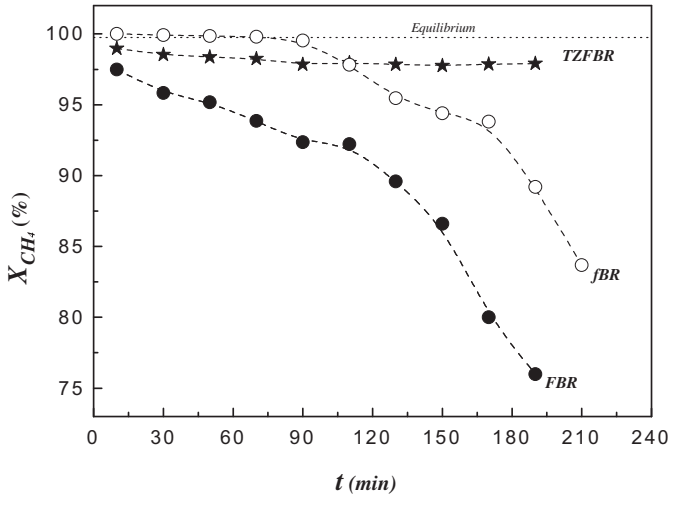

Fig. 3. Time evolution of methane conversion in different reactor configurations at $T = 850\ ^\circ C$ and $CH_4/H_2O/O_2 = 2/1.5/1$ (lines for visual help). Other operating conditions for fluidized bed reactors: $u_{r1} = 2.0$, $u_{r2} = 3.6$, $W_{cat} = 37.5$ g/zone, $W_{cat}/F = 6.3$ g min mmol^{-1}; for fixed bed reactor: $W_{cat} = 1$ g, $W_{cat}/F = 0.67$ g min mmol^{-1}.

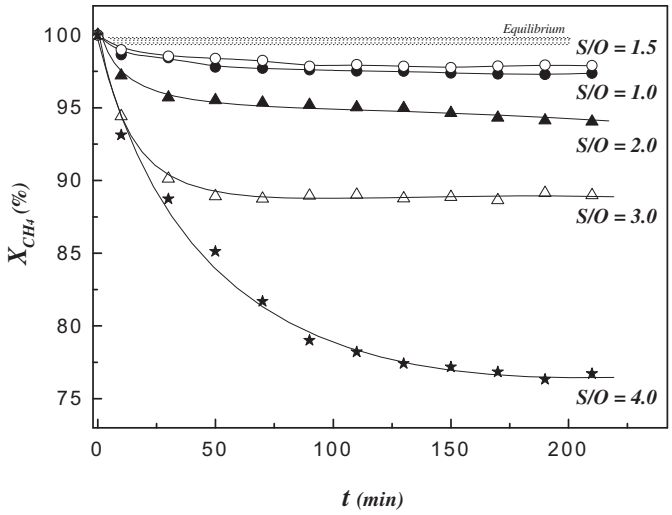

Fig. 4. Time evolution of methane conversion in the TZFBR for different steam to oxygen molar feed ratios at $CH_4/(H_2O + O_2) = 0.8$ (lines for visual help). Other operating conditions as for Fig. 3.

In order to analyse the catalyst state after reaction in these different reactor configurations, several solid samples were obtained from the bed after an experimental run and a cooling period fluidizing the bed with an inert gas stream. These samples are representative of the average state of the solid in the whole bed at the end of the run. Fig. 5 shows XRD patterns of these samples. It is observed that the peaks in the catalysts after reaction have a greater height–width ratio than the peaks in the fresh catalyst. Accordingly, it seems that the catalyst becomes more crystalline when it is used in reaction cycles. A slight increase in the size of the particles after reaction is also observed. In fact, a difference can be appreciated in the crystallinity of the catalyst before and after reaction. For example, if the peak of the Al_2O_3 at $2\theta = 67^\circ$ is observed, it can be seen that it is more intense in the catalysts after reaction. After use in both types of reactor, the peak in the catalysts appears at $2\theta = 26^\circ$ which corresponds with carbon. This peak is more intense in the catalyst after use in the FBR. In the catalysts after reaction peaks of Ni^0 are also observed (at $2\theta = 52^\circ$ and 76.3°), which do not appear in the fresh catalyst. The Ni^0 is the active phase

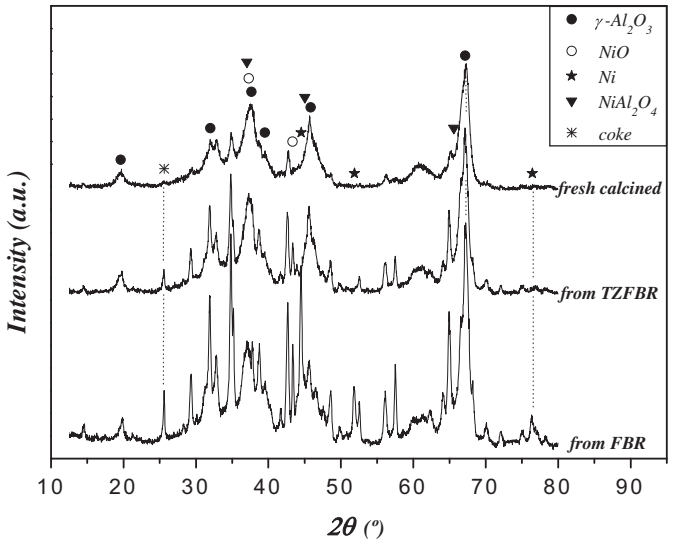

Fig. 5. XRD patterns of fresh and used 2.5%Ni/Al_2O_3 catalyst.

in the steam methane reforming and for this reason it is found in the catalysts after reaction. The freshly calcined catalyst sample is not reduced, so nickel is in the oxidized form (Ni^{2+}). It may be concluded that there are changes in the catalyst after use in both contact modes.

The BET specific surface areas (S_{BET}) of the different samples have also been analysed. A value of 59 $m^2\ g^{-1}$ was obtained for the freshly calcined catalyst, i.e. before reaction. When the reaction time increased, there was a reduction in the specific surface area for both types of reactor. A 38% loss in surface area was obtained for samples from the FBR with 60 h of time-on-stream, while 110 h was required to obtain the same percentage of surface area loss for the samples from the TZFBR. The coke formation in the pores and the sinterization process cause a reduction in the specific area.

TPR profiles of various samples (not shown) have been analysed in order to evaluate the catalyst reducibility. In the freshly calcined catalyst one very intensive peak was observed at around 800 °C and assigned to the $NiAl_2O_4$ spinel [34–36]. A series of peaks from 200 °C were related to the reduction of NiO [37]. After use in the FBR, the catalyst showed a main peak at 250 °C related to the NiO that interacts weakly with the support, and a series of peaks between 400 and 630 °C corresponding to the NiO highly dispersed in the Al_2O_3. All these peaks correspond to the reduction of NiO [38]. The catalyst TZFBR showed one peak at 410 °C corresponding to the reduction of free NiO and another at 620 °C corresponding to the reduction of NiO that weakly interacts with Al_2O_3. This is consistent with observations made in other works [39]. Comparing the three samples, it was observed that the freshly calcined catalyst is more difficult to reduce as the reduction peaks appear at a higher temperature than in the case of the catalysts after reaction.

According to the TEM images, the typical structure of alumina can be seen in the freshly calcined catalyst (Fig. 6a), but there are also other structures that may be due to the Ni-spinel. In Fig. 6b the presence of both types of structures can be observed. Ni particles are well dispersed in the material, the diameter of the crystallite being around 14 nm. In the case of the catalyst used in the FBR (Fig. 6c), coke formation in an agglomerated form was observed while dispersed Ni was not appreciated. On the other hand, in the catalyst used in TZFBR (Fig. 6d) the structure of the alumina remained and the presence of coke was not observed, neither in the form of nanofibers nor in the agglomerated form. The appearance is very similar to the catalyst before reaction, with the nickel well dispersed and a similar particle size. This corroborates the fact that using this contact mode resulted in no significant changes.

It can be concluded that in the TZFBR, the small stream of oxygen fed to the lower part of the fluidized bed was enough to continuously remove the coke that was formed in the methane reaction zone, achieving a steady state with a small amount of coke over the catalyst surface (depending on the S/O value, as previously seen). Furthermore, the process works in a mode different from that of conventional OSRM because in the reaction zone there is no oxygen, or only a small part of the oxygen inlet stream, present in the gas phase. This allows working in the reaction zone in a pseudo-SRM mode but with a reduced S/M ratio and in situ regeneration of the catalyst by coke combustion, resulting in a stable process. A comparison of results obtained in steady state from both reactor configurations is presented in the next section.

3.3. Comparison between TZFBR and FBR

The distribution of products was strongly influenced by the configuration of the reactor, as can be seen in Fig. 7. Hydrogen selectivity obtained in the TZFBR was slightly greater than in the FBR. Coke selectivity was approximately 10% in the FBR while there was no net coke formation with the TZFBR. Moreover, CO selectivity was higher in the case of the TZFBR, while the CO_2 selectivity was lower. This behaviour of the CO, CO_2 and coke selectivities could be due to the Boudouard reaction occurring to a greater extent in the FBR, and to the fact that methane combustion (where CO_2 is formed) is more important than partial oxidation (where CO is produced). Conversely, in the TZFBR coke combustion and gasification are favoured in the lower part of the bed by the oxygen + steam stream fed from the bottom of this reactor.

In this regard, the distribution of products from the TZFBR may depend on the relative size of the regeneration and the reaction zones of the bed. Fig. 8 shows a comparison of methane conversion and selectivity to hydrogen and to carbon monoxide for three different h_{CH_4}/H values. The experimental runs were carried out maintaining the total catalyst load in the bed and the inlet flowrates of methane, steam and oxygen at constant values. As can be seen in the figure, the selectivity to the desired products (H_2 and CO) has a maximum value at an intermediate h_{CH_4}/H ratio. When a lower value of this ratio was used, the oxygen stream was able to reach the reaction zone in which methane and SRM products were present, increasing the selectivity towards their combustion products (CO_2 and H_2O). In contrast, for a high value of the h_{CH_4}/H ratio the degree of catalyst regeneration was higher (i.e., lower coke content on the catalyst surface in the stationary state could be expected) and so a more active solid leading to higher conversions was obtained except when there was insufficient contact time in the reaction zone. When this occurs, the catalyst turns into a high oxidation state solid, being less selective for the SMR process (without oxygen in the gas phase) carried out in the reaction zone. Indeed, as noted by other authors [40,41], the increase in the degree of oxidation of the solid enhances the CO_2 formation at the expense of CO, whereas conversely the formation of the CO and H_2 products occurs preferentially over a reduced Ni/Al_2O_3 phase via reforming reactions of CH_4 with H_2O and CO_2 coming from the regeneration zone and/or produced in oxidation reactions (favoured over the NiO/Al_2O_3 phase).

Finally, Fig. 9 shows a comparison between TZFBR and FBR performances depending on the reactor temperature. As can be seen, there are huge differences in terms of activity and selectivity. In all the studies, the results obtained for the TZFBR in terms of methane conversion were stable and better than those for the FBR at a time-on-stream of $t = 190$ min, using the same catalyst load and the same operating conditions. It is worth mentioning that this

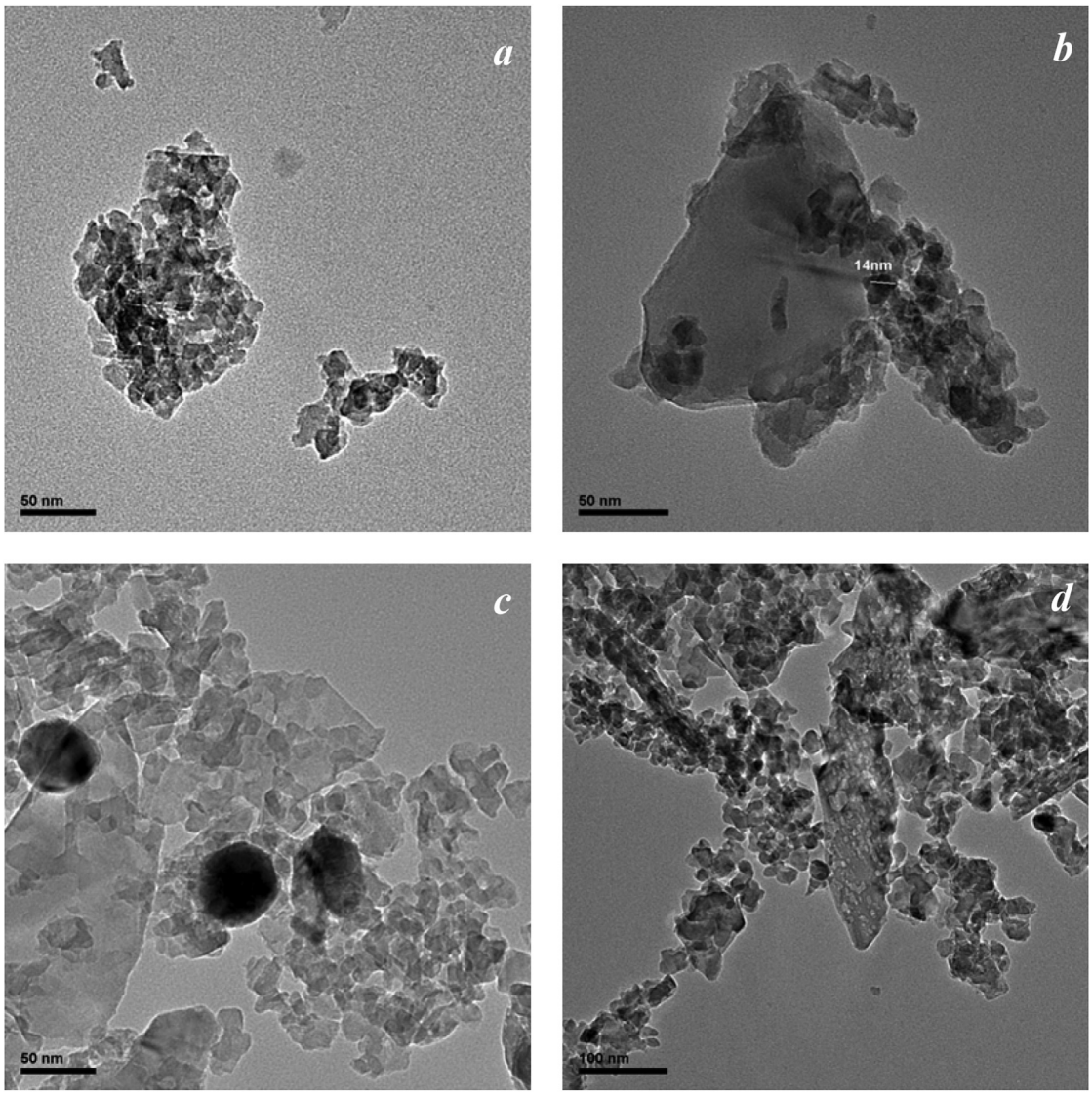

Fig. 6. TEM images of fresh and used 2.5%Ni/Al_2O_3 catalyst: a and b) fresh calcined, c) used in FBR, d) used in TZFBR.

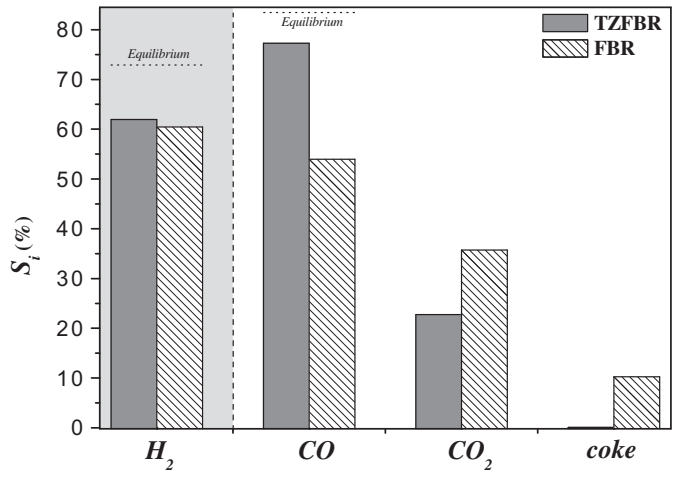

Fig. 7. Product distribution (as S_i values) from TZFBR and FBR at $t = 190$ min. Operating conditions as for Fig. 3. Coke is calculated by carbon mass balance closure.

stable behaviour was achieved working at low S/M molar feed ratios (S/M = 0.75 in the experiments shown in Fig. 9). In this respect, modern plants for hydrogen production from the hydrocarbon steam reforming process are normally designed for low steam/carbon ratios, typically 2.5 or less [42]. The advantage of working with low amounts of water is the reduction of the steam mass-flow rate through the plant and thus the diminishing of equipment size. However, steam/carbon ratios of 4 or 5 can result in higher hydrocarbon conversions and resolve the catalyst deactivation by coke deposition. In the TZFBR, stable high methane conversions have been achieved, approaching equilibrium (see Fig. 9) despite the very low S/M ratio.

Regarding the selectivity to products, it was possible to raise the CO selectivity using the TZFBR configuration, but the selectivity to H_2 remained analogous to that of conventional OSMR, i.e. using the FBR configuration. It is likely that the selectivity to hydrogen was not greater in this contact mode as a result of the reverse water-gas shift reaction (Eq. (4)) in which the hydrogen reacted with the CO_2 coming from the regeneration zone to produce water.

In any event, it may be concluded that the use of the TZFBR is an interesting route for hydrogen production from the oxidative steam

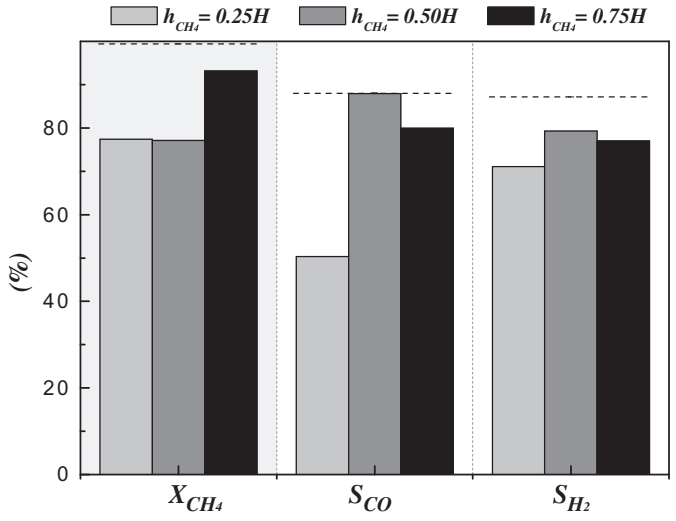

Fig. 8. Performance of SRM in the TZFBR (as X_{CH_4} and S_i values) at different h_{CH_4}/H ratios. W_{cat} = 75 g (H = 14 cm), $CH_4/H_2O/O_2$ = 2/2/0.5, t = 190 min. Other conditions as for Fig. 3.

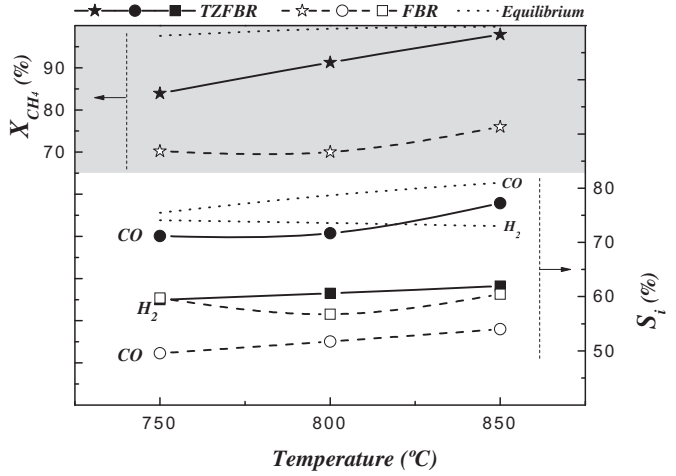

Fig. 9. Methane conversion and product distribution (as S_i values) from both FBR and TZFBR reactors as a function of temperature (lines for visual help). t = 190 min and other operating conditions as for Fig. 3.

reforming of methane, obtaining higher values of methane conversion and CO selectivity and an outlet stream richer in hydrogen than in the conventional OSRM configuration (i.e. cofeeding the three reagents into the catalytic bed). As a reference of the TZFBR performance, it can be calculated from Fig. 9 that a stable global yield to hydrogen $Y_{H_2/(CH_4+H_2O)}$ = 0.67 is obtained at 850 °C whereas in the FBR reactor only a $Y_{H_2/(CH_4+H_2O)}$ = 0.50 is obtained at the same temperature (moreover, this value will decrease with time-on-stream). In fact, the values of the global hydrogen yield from methane plus water obtained with the TZFBR exceed those reported in the literature for conventional reactors, even taking into account the non-stable performance of those traditional reactors.

4. Conclusions

A steady performance in the two zone fluidized bed reactor has been achieved in all the studied cases. A higher global yield to hydrogen has been observed in the TZFBR than in the FBR or fBR. In fact, the product distribution is also influenced by the reactor configuration, obtaining a higher hydrogen selectivity using the TZFBR. This is because the hydrogen obtained as product in the reaction zone is not in contact with the oxygen in gas phase. If some oxygen arrives in the reaction zone, its amount would be lower than in the case of the experiments carried out with the other reactor configurations. Moreover, working with the fBR or the FBR there is always some coke selectivity, while with the TZFBR there was no net coke formation. With the FBR, CO selectivity was lower than with the TZFBR, while CO_2 selectivity was higher because the Boudouard reaction and methane combustion took place to a greater extent while the reverse water-gas shift reaction occurred to a lesser extent.

The use of the TZFBR also provides better values of methane conversion than the FBR working with the same conditions, due to a better regeneration of the catalyst which continuously eliminates the coke.

Acknowledgements

This work has been partially funded by the Spanish Ministry of Education and Science (project CTQ 2007-63420). Financial aid for the maintenance of the consolidated research group CREG has been provided by the Fondo Social Europeo (FSE) through the Gobierno de Aragón (Aragón, Spain). L. Pérez-Moreno also thanks the Gobierno de Aragón for a grant.

References

[1] N. Bion, F. Epron, D. Duprez, in: J.J. Spivey, K.M. Dooley (Eds.), Catalysis, vol. 22, 2010, pp. 1–55.
[2] M. Nurunnabi, B. Li, K. Kunimori, K. Suzuki, K. Fujimoto, K. Tomishige, Appl. Catal., A: Gen. 292 (2005) 272–280.
[3] A.F. Lucrédio, E.M. Assaf, J. Power Sources 159 (2006) 667–672.
[4] C.H. Bartholomew, Appl. Catal. 107 (1993) 1–57.
[5] M. Nurunnabi, Y. Mukainakano, S. Kado, T. Miyazawa, K. Okumura, T. Miyao, S. Naito, K. Suzuki, K.I. Fujimoto, K. Kunimori, K. Tomishige, Appl. Catal., A: Gen. 308 (2006) 1–12.
[6] M.N. Pedernera, J. Piña, D.O. Borio, Chem. Eng. J. 134 (2007) 138–144.
[7] J.M. Ginsburg, J. Piña, T. El Sohl, H.I. de Lasa, Ind. Eng. Chem. Res. 44 (2005) 4846–4854.
[8] D.L. Trimm, Catal. Today 49 (1999) 3–10.
[9] K. Takehira, T. Shishido, D. Shoro, K. Murakami, M. Honda, T. Kawabata, K. Takaki, Catal. Commun. 5 (2004) 209–213.
[10] K. Takehira, T. Shishido, P. Wang, T. Kosaka, K. Takaki, J. Catal. 221 (2004) 43–54.
[11] J.A.C. Dias, J.M. Assaf, J. Power Sources 130 (2004) 106–110.
[12] S. Freni, G. Calogero, S. Cavallaro, J. Power Sources 87 (2000) 28–38.
[13] B.T. Li, K. Maruyama, M. Nurunnabi, K. Kunimori, K. Tomishige, Ind. Eng. Chem. Res. 44 (2005) 485–494.
[14] K. Tomishige, S. Kanazawa, K. Suzuki, M. Asadullah, M. Sato, K. Ikushima, K. Kunimori, Appl. Catal., A: Gen. 233 (2002) 35–44.
[15] K. Tomishige, M. Nurunnabi, K. Maruyama, K. Kunimori, Fuel Process. Technol. 85 (2004) 1103–1120.
[16] B. Li, K. Maruyama, M. Nurunnabi, K. Kunimori, K. Tomishige, Appl. Catal., A: Gen. 275 (2004) 157–172.
[17] B. Li, R. Watanabe, K. Maruyama, K. Kunimori, K. Tomishige, Catal. Today 104 (2005) 7–17.
[18] K. Yoshida, N. Begum, S. Ito, K. Tomishige, Appl. Catal., A: Gen. 358 (2009) 186–192.
[19] K. Tomishige, S. Kanazawa, M. Sato, K. Ikushima, K. Kunimori, Catal. Lett. 84 (2002) 69–74.
[20] K. Tomishige, S. Kanazawa, S. Ito, K. Kunimori, Appl. Catal., A: Gen. 244 (2003) 71–82.
[21] B. Li, S. Kado, Y. Mukainakano, M. Nurunnabi, T. Miyao, S. Naito, K. Kunimori, K. Tomishige, Appl. Catal., A: Gen. 304 (2006) 62–71.
[22] B. Li, S. Kado, Y. Mukainakano, T. Miyazawa, T. Miyao, S. Naito, K. Okumura, K. Kunimori, K. Tomishige, J. Catal. 245 (2007) 144–155.
[23] Y. Mukainakano, B. Li, S. Kado, T. Miyazawa, K. Okumura, T. Miyao, S. Naito, K. Kunimori, K. Tomishige, Appl. Catal., A: Gen. 318 (2007) 252–264.
[24] Y. Mukainakano, K. Yoshida, K. Okumura, K. Kunimori, K. Tomishige, Catal. Today 132 (2008) 101–108.
[25] Y. Mukainakano, K. Yoshida, S. Kado, K. Okumura, K. Kunimori, K. Tomishige, Chem. Eng. Sci. 63 (2008) 4891–4901.
[26] J. Herguido, M. Menéndez, J. Santamaría, Catal. Today 100 (2005) 181–189.
[27] R. Ramos, J. Herguido, M. Menéndez, J. Santamaría, J. Catal. 163 (1996) 218–221.
[28] C. Callejas, J. Soler, J. Herguido, M. Menéndez, J. Santamaría, Stud. Surf. Sci. Catal. 130 (2000) 2717–2722.

[29] M.P. Lobera, C. Téllez, J. Herguido, M. Menéndez, Appl. Catal., A: Gen. 349 (2008) 156–164.
[30] M.P. Lobera, C. Téllez, J. Herguido, M. Menéndez, Ind. Eng. Chem. Res. 48 (2009) 6573–6578.
[31] L. Pérez-Moreno, J. Soler, J. Herguido, M. Menéndez, Ind. Eng. Chem. Res. 51 (2012) 8840–8848.
[32] M. Nurunnabi, Y. Mukainakano, S. Kado, T. Miyao, S. Naito, K. Okumura, K. Kunimori, K. Tomishige, Appl. Catal., A: Gen. 325 (2007) 154–162.
[33] D.C.R.M. Santos, L. Madeira, F.B. Passos, Catal. Today 149 (2010) 401–406.
[34] J.I. Villacampa, C. Royo, E. Romeo, J.A. Montoya, P. Del Angel, A. Monzón, Appl. Catal., A: Gen. 252 (2003) 363–383.
[35] A.L. Alberton, M.M.V.M. Souza, M. Schmal, Catal. Today 123 (2007) 257–264.
[36] Z. Hao, Q. Zhu, Z. Jiang, B. Hou, H. Li, Fuel Process. Technol. 90 (2009) 113–121.
[37] H.T. Jiang, H.Q. Li, Y. Zhang, J. Fuel Chem. Technol. 35 (2007) 72–78.
[38] H. Li, Y. Xu, C. Gao, Y. Zhao, Catal. Today 158 (2010) 475–480.
[39] Y. Song, H. Liu, S. Liu, D. He, Energy Fuels 23 (2009) 1925–1930.
[40] D. Dissanayake, M.P. Rosynek, K.C.C. Kharas, J.H. Lunsford, J. Catal. 132 (1991) 117–127.
[41] H. Provendier, C. Petit, A. Kiennemann, C.R. Acad. Sci. 4 (2001) 57–66.
[42] C. Pistonesi, A. Juan, B. Irigoyen, N. Amadeo, Appl. Surf. Sci. 253 (2007) 4427–4437.

Symbols

FBR: conventional fluidized bed reactor
fBR: fixed bed reactor
F_i: molar flow of product i (mmol min^{-1})
h: bed height (cm)
H: total bed length (cm)
h_{CH_4}: methane feed point (cm)
n_i: number of C atoms in molecule of product i
OSRM: oxidative steam reforming of methane
S/M: steam to methane molar feed ratio (−)
S/O: steam to oxygen molar feed ratio (−)
S_i: selectivity from methane to product i as defined in Eqs. (10) and (11) (%)
SRM: steam reforming of methane
T: temperature in the bed (°C)
t: time on stream (min)
TZFBR: two zone fluidized bed reactor
u: gas velocity in the bed (cm min^{-1})
u_{mf}: minimum fluidization velocity (cm min^{-1})
u_r: relative gas velocity defined as u/u_{mf} (−)
u_{r1}: relative gas velocity at the entry of the regeneration zone in TZFBR (−)
u_{r2}: relative gas velocity at the entry of the reaction zone in TZFBR (−)
W_{cat}: mass load of catalyst in the bed (g)
X_{CH_4}: Fractional conversion of methane as defined in Eq. (9) (%)
$Y_{H_2/(EtOH+H_2O)}$: global yield to hydrogen as defined in Eq. (12) (−)

Superscripts
in: at the reactor entrance
out: at the reactor exit